

Effect of Molarity on Microstructural, Structural and Optical Properties of ZnO Thin Films Prepared by Ultrasonic Atomization and Pyrolysis Technique

S. D. Bagul*, D. G. Patil

P.G. Dept. of Physics, Pratap College (Autonomous), Amalner, Dist. Jalgaon

*Corresponding author: Dr. S.D.Bagul

Abstract: Nanostructured ZnO thin films were prepared using ultrasonic atomizer and pyrolysis technique by changing molarity of ZnCl₂ solution. 0.1M (300ml) stock solution was converted into fine mist droplets using ultrasonic atomizer (Gapsol 9001 RBI Meylan, France with frequency of operation 2.1-2.3MHz). The fine mist was allowed to pass and pyrolyzed onto previously kept glass substrates in horizontal quartz reactor heated using double zone furnace at 500°C. The thin film so prepared was termed as S1. Repeating above procedure, films S2, S3 and S4 were prepared using ZnCl₂ solutions of molarities respectively 0.05M, 0.025M and 0.01M. The structural and microstructural properties of the films were studied using XRD and FESEM. Thickness of the film was measured by cross-sectional view of FESEM image. The optical properties of the films were characterized using UV-Visible and Photoluminescence (PL) spectroscopy. The results are discussed and interpreted.

Keywords: Zinc oxide, Ultrasonic atomization and Pyrolysis, Thin films, Vertically grown bundles of Nanorods

1. INTRODUCTION

The ZnO is highly functional material for science and technology. The world requires large quantity of nanocrystalline ZnO either in thin film or powder form. The ZnO has high mobility of conduction electrons and good chemical and thermal stability [1,2]. It is a direct band gap wurtzite -type semiconductor. In nanoparticulate materials, the enhanced surface area and interconnected particles give rise to a large number of energy traps on the surface and grain boundaries [3-6].

The present paper report a simple technique to prepare porous and nanocrystalline ZnO thin films with different molarity. The preparative conditions of the thin films were optimized so as to obtain highly textured ZnO thin

films. The prepared thin films were studied for its structural, microstructural and optical properties. Ultrasonic atomization and pyrolysis technique was used for thin film preparation. It is easier technique to produce highly textured porous thin films, requiring no vacuum for processing than other coating methods. Additionally, this coating technique features the ability to control desired morphology characteristics. Uniform, thin, well textured and crack free thin films with high transmittance and conductive properties are possible using coating by pyrolysis. The technique used here produces highly uniform film because the pressure inside the quartz reactor furnace is maintained by the trap system at rear end. Mist of the solution is flowed uniformly on the surface of the substrates which are placed inline the quartz reactor at particular temperature.

2. Experimental

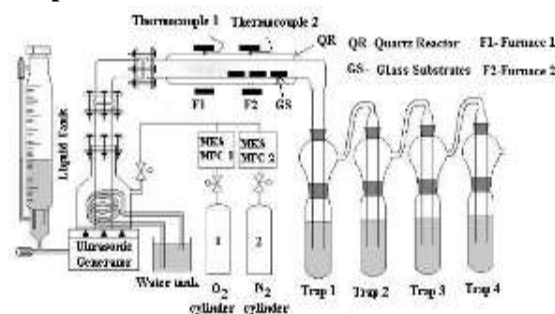


Fig. 1. Ultrasonic atomization and pyrolysis system to prepare thin films

The ultrasonic atomization and pyrolysis system is shown in Fig.1 [7]. It consists of ultrasonic atomizer (Gapsol 9001 RBI Meylan, France with frequency of 2.1-2.3MHz), double zone quartz reactor, furnace, thermocouple with temperature indicator and trap system. Ultrasonic generator produces high frequency waves having frequency of 2.1-2.3MHz. This high frequency signal is supplied to piezoelectric transducers. The transducers convert a high frequency into mechanical energy. This energy is used to convert the precursor solution into the fine mist or smoke.

The mist is pushed into the quartz reactor placed into horizontal furnace by air compressor connected to chamber of ultrasonic generator. The mist was pyrolyzed onto the previously kept glass substrates in horizontal furnace.

2.1. Preparation of ZnO thin films

Ultrasonic atomization and pyrolysis technique (Fig.1) was used to prepare nanocrystalline ZnO thin films. In a typical synthesis, 0.1M ZnCl₂ solution (300 ml) was prepared in double distilled water and 0.1 ml HCl was added so as to get clear solution. This stock solution was stored into vertical cylindrical flask connected to ultrasonic atomizer. Ultrasonic atomizer was used to convert the solution into mist of fine droplets. The mist droplets were pushed using pressurized air from air compressor into horizontal quartz reactor placed into the double zone horizontal furnace. The glass substrates were placed into the quartz reactor (in IInd zone of the furnace) so that mist particles could pass from the top of the glass substrates and be pyrolyzed. The carrier airflow rate was optimized as 20kg/cm² to prevent segregation of mist droplets. The Ist and IInd zones of the furnace were kept respectively at 200°C and at 500°C. In first zone, the water from mist droplets would be removed partially and in second zone mists would be pyrolyzed on glass substrates. The mist droplets were passed for optimized time interval of 30 minute to get uniform thin films. Due to trapping system attached to rear end of reactor, the rate of flow of mist was uniformly controlled which would help to get highly uniform thin films [7]. After successful deposition, the films were removed and fired at 500°C for 1 hour in muffle furnace. The ZnO thin films so prepared (0.1M) were termed as S1. Repeating the same procedure, ZnO thin films samples S2, S3 and S4 were prepared using ZnCl₂ solution of molarity respectively 0.05M, 0.025M and 0.01M.

3. Results and discussion

3.1. Crystalline structure of ZnO thin films

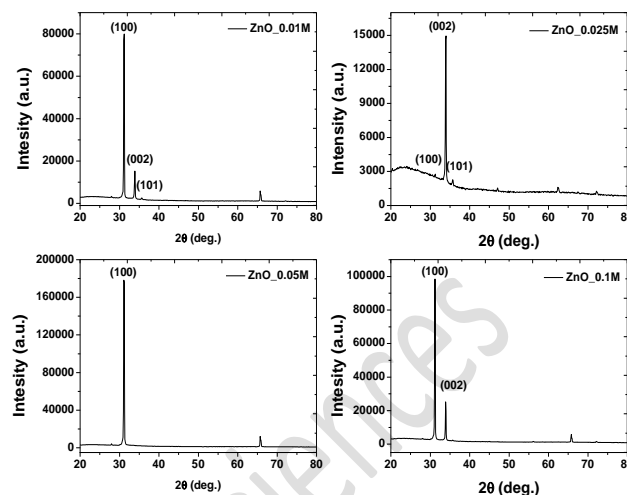


Fig. 2: XRD patterns of the ZnO thin films prepared using ZnCl₂ solutions of different molarities

Table 1: Dependence of size and shape of ZnO crystallites in the films on molarity

Sample name	Molarity ZnCl ₂ solution	Crystallite size (nm)
S1	0.1M	59.36
S2	0.05M	58.10
S3	0.025M	52.60
S4	0.01M	51.21

Fig.2 shows the XRD patterns of the films prepared using ZnCl₂ solutions of different molarities:0.01M,0.025M, 0.05M and 0.1M. The XRD patterns of the films are matching well with the standard data of ZnO with JCPDS file no.01-070-8072. Average size of crystallites associated with S1, S2, S3 and S4 ZnO thin film samples were determined using Scherrer equation. Average crystallite size and shapes were observed to be dependent on the molarity of ZnCl₂ solution as presented in Table 1.

3.2. Microstructural studies of S2 and S3 thin films using FESEM images

3.2.1 Cross sectional view of S3 thin film

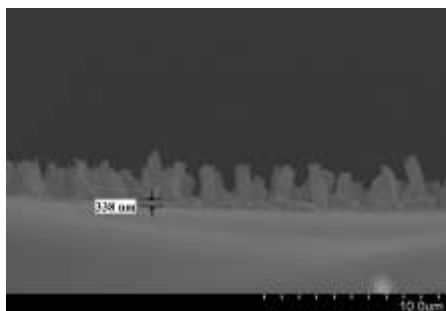
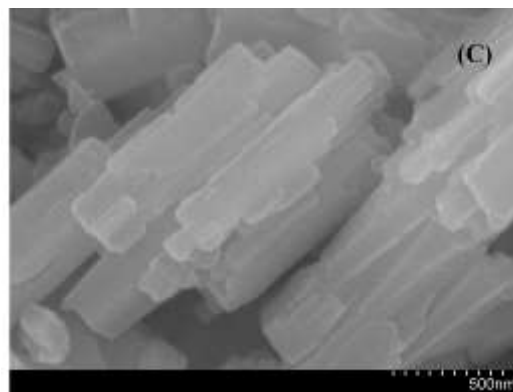
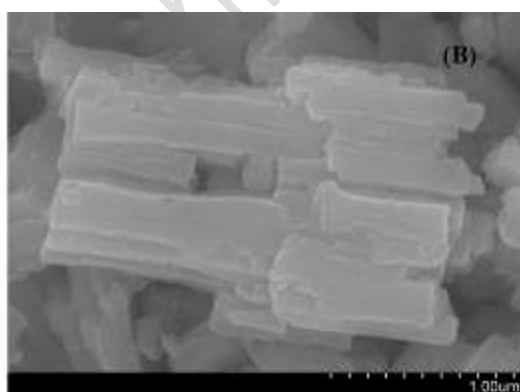
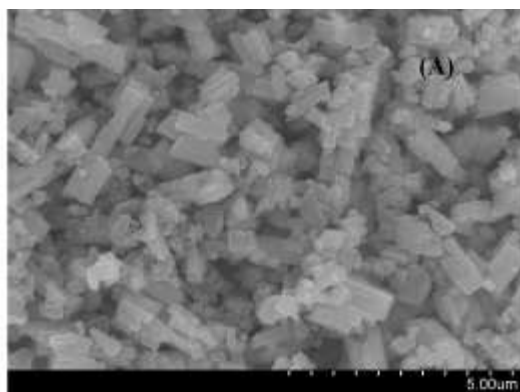


Fig. 3: FESEM image: Cross sectional view of thin film S3

FESEM image in Fig.3 shows cross sectional view of sample S3. The thickness of S3 thin film was found to be 338 nm. Vertical bundles of rods are clearly seen in the image.

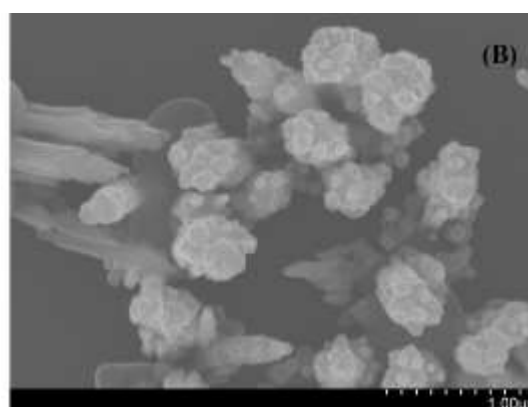
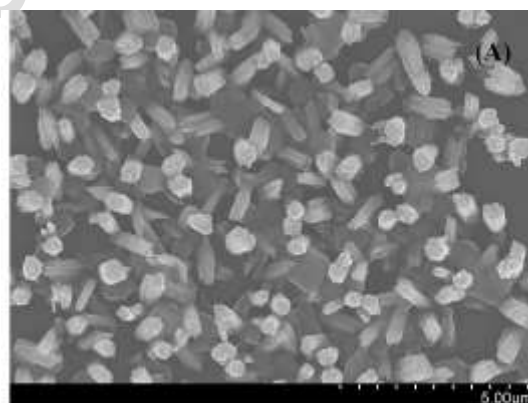
3.2.2 Topography and Morphology of crystallites in S2 film

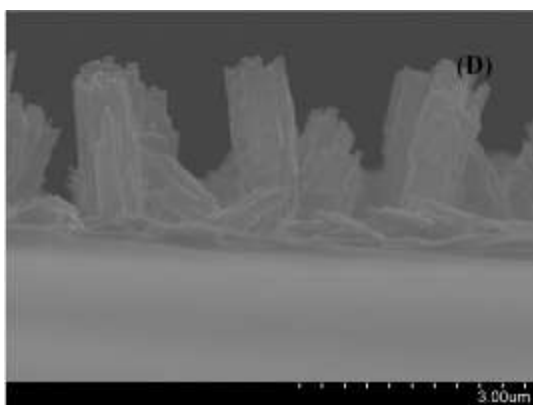
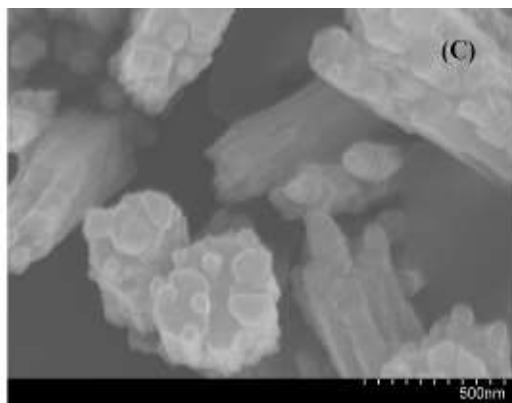


Figs. 4(A), (B), (C): FESEM images of thin film sample S2

Figures 4(A),(B),(C) show FESEM images (at different magnifications) of sample S2 prepared using $ZnCl_2$ solution of molarity of 0.05M. The bundles of nanorods are observed to be randomly distributed horizontally on the film surface. No rod is found to be vertically grown. The size of rods is observed to be of the order of micrometer.

3.2.3 Topography and Morphology of crystallites in S3 film





Figs. 5(A),(B),(C) and (D): FESEM images of thin film sample S3

Figures 5(A), (B), (C) and (D) show FESEM images (at different magnifications) of sample S3 prepared using ZnCl₂ solution of molarity of 0.025M. The bundles of nanorods are observed to be randomly distributed on the film surface. Most of the rods on surface of the film are seen to be vertically grown as against the horizontal rods in sample S2. Very few rods are found to be horizontally grown. The size of rods is observed to be of the order of micrometer. It is clearly seen from FESEM images of S2 and S3 samples that average diameter of the ZnO rod decreases with the decrease in molarity.

3.4. UV-Visible spectroscopy of ZnO thin film samples

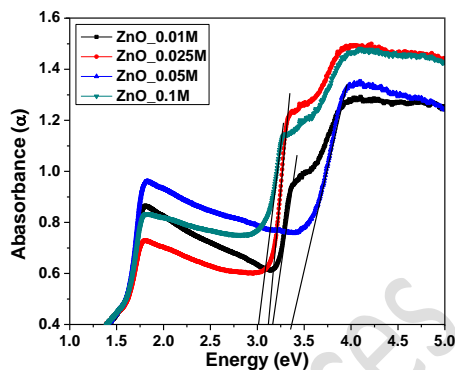


Fig. 6: UV-Visible absorption spectra of S1, S2, S3 and S4 samples

Optical absorption spectra of ZnO thin film S1, S2, S3 and S4 samples are depicted in Fig. 6. The edge of absorbance is observed in the region of 4.2-3.0 eV for the films. The absorption edge is observed to be shifted towards smaller wavelength side with the decrease in concentration of ZnCl₂ solution. This indicates that there is increase of optical band gap with the decrease in concentration of ZnCl₂ solution. This phenomenon is known as blue shift. The values of optical band gap energy of the ZnO thin films determined from the absorption spectra are tabulated in Table 2.

Table 2: Optical band gap

Molarity ZnCl ₂ solution	Eg-Band gap energy (eV)
0.1M	3.02
0.05M	3.38
0.025M	3.12
0.01M	3.18

The optical band gap energy of ZnO thin film S2 was found to be largest as compared to band gap energies of samples S1, S3 and S4. It may be due to high crystallinity of the film as we can see from the XRD patterns of the films.

3.5. Photoluminescence spectroscopy

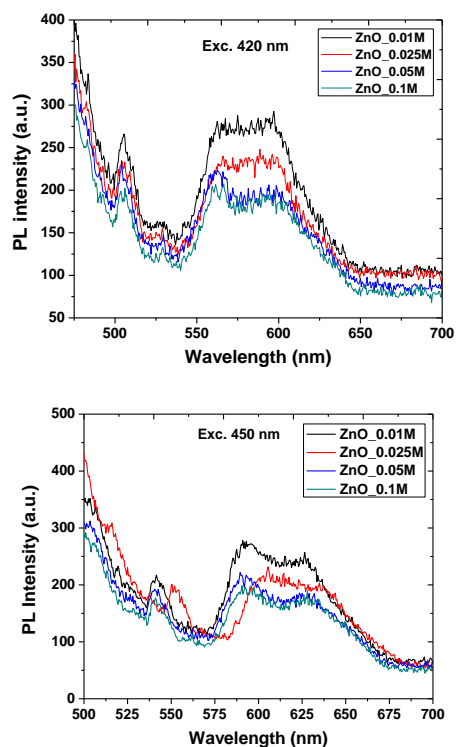


Fig.7: Photoluminescence (PL) emission spectra

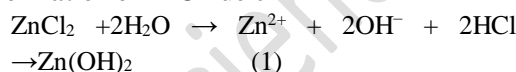
Fig.7 (A) and (B) shows room temperature photoluminescence (PL) spectra carried out at two excitation wavelengths: 420nm and 450 nm respectively. To measure the surface defects of the thin films, broad emission PL spectra shows emission peaks at 566, 562, 588, and 597 nm respectively for S1, S2, S3 and S4 which are the visible range of solar spectrum. The emission peaks may be caused due to surface defects (such as interstitial of metals and oxygen vacancies) in ZnO the thin films [8, 9]. It is seen from the PL spectra that the intensity of emission peaks increase with decrease in molarity of ZnCl₂ which in turn may be due to decrease in crystallite size of ZnO.

4. Discussion

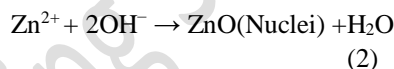
In general, the wurtzite ZnO crystal has two polar planes: the low index planes that have high surface energy and in the metastable status. In addition, with the wurtzite hexagonal crystal structure, the six crystallographic equivalent nonpolar planes (parallel to the c-axis) are more stable due to relatively low surface energy [10]. The formation of various shapes of ZnO nanocrystals is originated in the relative growth rates of different crystal facets. There is a large difference in growth rates of the wurtzite hexagonal ZnO crystals in different directions. According to

the lowest energy principle, hexagonal ZnO crystals are inclined to grow along the [0001] facet to achieve the surface energy minimization, hence the growth velocity along the [0001] direction is faster than other growth facets, which lead to the formation of nanorods along the c-axis. The morphology of ZnO nanostructure can be tuned by changing the growth parameters such as precursor's ion concentration and the size and length of ZnO nanorods can be easily controlled during the chemical process. It can be seen from the SEM images in **Figs.: 4 and 5** that ZnCl₂ concentration has a great influence on the morphology of the ZnO nanorods.

(i) Formation of ZnO nuclei



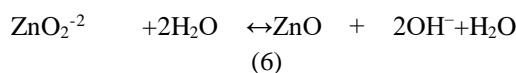
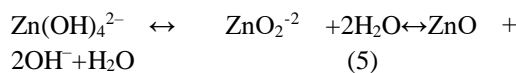
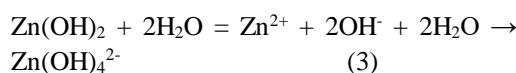
or



(ii) Growth-Dissolution

Recrystallization:

Subsequently, ZnO nanostructures undergo a reversible dissolution and recrystallization process via formation of Zn(OH)₂, leading to formation of one dimensional (1D) ZnO microrods.



The formation mechanism of the ZnO nanostructures is a complex process and mostly considered to include two main steps: the formation of growth units (the generation of a ZnO nuclei) and the incorporation of growth units into crystal lattice of the ZnO nanocrystals (subsequent ZnO crystal growth). Zn(OH)₄²⁻ complexes serve as basic growth units for the formation of ZnO nanostructures [11-12]. When the concentration of Zn²⁺ and OH⁻ reaches to supersaturation, ZnO nuclei form according to

reaction no 1 and 2. During the process, part of the $Zn(OH)_2$ colloids dissociate into Zn^{2+} and OH^- according to reaction no 4. When the concentration of these growth units ($Zn(OH)_4^{2-}$ complexes) exceeds the critical supersaturation level, the growth units become ZnO nuclei spontaneously in the solution.

In an aqueous solution, the formed $Zn(OH)_2$ clusters dissolve in Zn^{2+} and OH^- ions due to plenty of OH^- ions. The growth units ($Zn(OH)_4^{2-}$ complexes) being relatively more unstable as compared to ZnO nuclei, they would be transported to the surface of ZnO nuclei where it would be dehydrated. The rate of ZnO nucleation and transportation of growth units would be slow and systematic. ZnO is a polar material. Zinc and oxygen atoms are arranged alternatively along the c-axis. The growth rate along c-axis is faster than those along other directions. Thus, growth of ZnO nuclei occurs preferentially along the c axis of wurtzite structure ([0001] direction) to form rod-like structures.

5. Summary and Conclusions

- ZnO thin films were prepared successfully by changing molarity (as: 0.1M, 0.05M, 0.025M and 0.01M) using ultrasonic atomization and pyrolysis technique.
- The FESEM images of ZnO thin films revealed that the topology changed due to change in preparative conditions (molarity as: 0.1M, 0.05M, 0.025M and 0.01M).
- The bundles of nanorods were observed to be randomly distributed with their orientation parallel to the film surface when film was prepared from $ZnCl_2$ solution of molarity of 0.05M. No rod was found to be vertical on the film surface.
- Most of the rods on surface of the film are seen to be vertical (perpendicular to the film surface) when film was prepared from $ZnCl_2$ solution of molarity of 0.025M. Such films are reported to be technologically important and attractive.
- The size of crystallites associated with films was observed to be dependent on molarity of the precursor solution.
- The band gap energy of the films was observed to be dependent on molarity of the precursor solution.

- The absorption edge was found to be shifted to lower wavelength side, that is, there was blue shift due to nanocrystalline nature of the associated crystallites.
- Photoluminescence peaks in PL spectra of the films were observed to in visible range of solar spectrum.

Acknowledgements

The authors are thankful to the Head, Department of Physics and Principal, Pratap College, Amalner for providing laboratory facilities for this work.

References

- [1] T. Seiyama, A. Kato, K. Fujiishi, M. Nagatani, A new detector for gaseous components using semiconductive thin films, *Anal. Chem.* 34 (1962) 1502–1503.
- [2] N. Yamazoe, G. Sakai, K. Shimano, Oxide semiconductor gas sensors, *Catal. Surveys Asia* 1 (2003) 63–75.
- [3] T. L. Thompson, J. T. Yates, Surface Science Studies of the Photoactivation of TiO_2 — New Photochemical Processes, *Chem. Rev.* 106 (2006) 4428–4453.
- [4] J. Nelson, R. E. Chandler, Random walk models of charge transfer and transport in dye sensitized systems, *Coord. Chem. Rev.* 248 (2004) 1181–1194.
- [5] A. Fujishima, X. Zhang, D. A. Tryk, TiO_2 photocatalysis and related surface phenomena, *Surf. Sci. Rep.* 63 (2008) 515–585.
- [6] M. J. Elser, T. Berger, D. Brandhuber, J. Bernardi, O. Diwald, E. Knözinger, Particles Coming Together: Electron Centers in Adjoined TiO_2 Nanocrystals, *J. Phys. Chem. B* 110 (2006) 7605–7608.
- [7] L.A. Patil, M.D. Shinde, A.R. Bari, V.V. Deo, Novel trapping system for size wise sorting of SnO_2 nanoparticles synthesized from pyrolysis of ultrasonically atomized spray for gas sensing, *Sens. Actuators B* 143 (2009) 316–324.
- [8] M. D. McCluskey, S. J. Jokela, “Defects in ZnO,” *Journal of Applied Physics*, vol. 106, no. 7, pp. 071101-071113, 2009.
- [9] S. Ilcan, Y. Caglar, M. Caglar, (Preparation and characterization of ZnO thin films deposited by sol-gel spin

- coating method), J. Optoelectron.
Adv. Mater., 10, (2008), 2578-2583.
- [10] Vayssieres, L., Keis, K., Hagfeldt, A. and Lindquist, S. E., Chemistry of Materials, 13(12)(2001) pp. 4395-4398.
- [11] Venkateswarlu, K., Sreekanth, D., Sandhyarani, M., Muthupandi, V., Bose, A. C. and Rameshbabu, N., International Journal of Bioscience, 2(6)(2012) pp. 389-393.
- [12] Polsongkram, D., Chamninok, P., Pukird, S., Chow, L., Lupan, O., Chai, G., Khallaf H., Park, S. and Schulte, A., Physica B 403(2008)(19-20), pp. 3713-3717.

Journal of Engineering Sciences